

## Chaos in a resonantly kicked oscillator

This article has been downloaded from IOPscience. Please scroll down to see the full text article.

1995 J. Phys. A: Math. Gen. 28 2515

(<http://iopscience.iop.org/0305-4470/28/9/013>)

View [the table of contents for this issue](#), or go to the [journal homepage](#) for more

### Download details:

IP Address: 171.66.16.68

The article was downloaded on 02/06/2010 at 01:29

Please note that [terms and conditions apply](#).

# Chaos in a resonantly kicked oscillator

Mark V Daly† and Daniel M Heffernan†‡

† Department of Mathematical Physics, St Patrick's College, Maynooth, Co Kildare, Ireland  
and School of Physical Sciences, Dublin City University, Dublin 9, Ireland

‡ School of Theoretical Physics, Dublin Institute of Advanced Studies, Dublin 4, Ireland

Received 22 April 1994, in final form 10 February 1995

**Abstract.** We study, in detail, the structure of the stochastic layer of a resonantly kicked oscillator. For the resonantly kicked case the stochastic layer has a crystalline or quasicrystalline structure depending on the parameter  $\omega_0\tau = 2\pi n/m$ , where  $\tau$  is the kicking period,  $2\pi/\omega_0$  the natural period of the oscillator and  $n$  and  $m$  are integers. For this resonant case we obtain the underlying orbit structure and the exact mechanism responsible for the diffusion in phase space is established. The diffusion of orbits in the stochastic layer is examined and a general universal form for the diffusion coefficient obtained.

## 1. Introduction

In dissipative systems one can completely characterize chaos from a knowledge of the unstable periodic orbits [1, 2]. In both classical and quantum chaos knowledge of the orbit structure is fundamental and has proved extremely useful in untangling and quantifying the dynamical properties of the system [1, 3, 4]. In the problem we treat below we show that knowledge of the orbit structure in phase space enables one to characterize chaos in the forced oscillator and obtain a detailed understanding of the mechanism of diffusion in the stochastic layer of the system. Such detailed knowledge enables one to gain insight into quantum chaos and to understand in a quantitative way what is meant by diffusion in quantum chaos problems.

The model we study below is a fundamental one, both in classical and quantum physics [5, 6]. The nonlinearly kicked harmonic oscillator can be related directly back to the kicked rotator [7, 8] by letting the natural period of oscillation of the oscillator tend to zero. We show that for a wide range of parameters, much larger than one would expect, the results obtained for the kicked rotator can be applied to this system with little or no modification emphasizing the similarity and the connection between the two systems. In recent years a related model, which was originally introduced as a first-order approximation to the fourth-order Poincaré map of the kicked harmonic oscillator when the kick strength is very much less than one, has undergone extensive analysis [9, 10]. This kicked Harper model has recently been shown by Dana to have an *exact* relationship to the kicked harmonic oscillator for general *even* potentials (see [10, 11]). The importance of the kicked Harper model is that it has been shown to exhibit quantum suppression of diffusion on the stochastic webs under specific circumstances [10]. Although these conditions for suppression are quite specific, the importance of this suppression and the relevance of this system to the kicked oscillator is currently a very active area of research both in the classical and quantum limit [10, 12–14].

In the problem that we study below, under the condition of resonant kicking, the stochastic layer has a crystalline or quasicrystalline structure depending on the parameter

$\omega_0\tau = 2\pi n/m$ , where  $\tau$  is the kicking period,  $2\pi/\omega_0$  the natural period of the oscillator and  $n$  and  $m$  are integers. It has been postulated by Berman [6] that with the presence of an extra time scale ( $\propto \ln(\hbar^{-1})$ ) in the quantum regime, the quantum analogue of the crystalline structure in phase space might allow for the possibility of the non-suppression of chaos, that is the delocalization of the quantum wavefunctions, and hence the nonlinearly kicked oscillator model would be a simple example where there would be quantum chaos. It has become necessary to obtain a more detailed and quantitative understanding of the mechanism of diffusion in both the classical and quantum limits. *In this paper we report on the detailed analysis of the mechanism of diffusion in the classical limit for the resonantly kicked case.* The quantum version of the model is currently under active study [6, 14].

The main thrust of this paper is to use the orbit structure of the phase space of the nonlinearly resonantly kicked harmonic oscillator to analyse the dynamical properties of this system classically. We examine in detail the case when  $\omega_0\tau = 2\pi n/m$ . Using the appropriate return map, we can show the existence of an infinite grid of hyperbolic points over the whole 2D plane of the phase space and we show how some orbits can diffuse over the whole phase space as a consequence. We also present a form of the driving term which allows explicit prediction of orbits on or near the stochastic layer boundary. The layer itself is analysed with its width measured and compared to theoretical predictions [5, 15]. The diffusion of orbits in the stochastic layer is examined and a general form for the diffusion coefficient given which is independent of the periodicity of the system's phase space. To our knowledge this is the first detailed study of the orbit structure and resonant tori breakup in the resonantly kicked case.

## 2. The model

The model we have chosen to study in detail is a quantum harmonic oscillator in the presence of a nonlinear kicking potential  $V(p, q)$  whose time dependence is governed by the periodic delta function [6]

$$H_T(t) = \frac{p^2}{2M} + \frac{1}{2}M\omega_0^2q^2 + V(p, q) \sum_{n=-\infty}^{\infty} \delta(t - n\tau) \quad (1)$$

where

$$V(p, q) = \mu_Q \cos(kq). \quad (2)$$

This model and related driven systems are fundamental to a wide range of disciplines in classical and quantum physics [16–22].  $\mu_Q$  is the parameter which governs the strength of kicking and hence the richness of the system's dynamics (that is the degree of non-integrability). This choice preserves the space inversion parity  $P$  and time reversal  $T$  of the original Hamiltonian  $H$ . The addition of the potential term  $V(p, q)$  means that the system is non-integrable and possesses highly complex dynamics.

The mapping obtained from the Hamiltonian above is

$$x(n+1) = x(n) \cos(\omega_0\tau) + y(n) \sin(\omega_0\tau) + \mu_{cl} \sin(2Kx(n)) \sin(\omega_0\tau) \quad (3)$$

$$y(n+1) = y(n) \cos(\omega_0\tau) - x(n) \sin(\omega_0\tau) + \mu_{cl} \sin(2Kx(n)) \cos(\omega_0\tau) \quad (4)$$

where

$$K = \epsilon/\epsilon_0 \quad \beta = \omega_0\tau \quad \text{and} \quad \mu_{cl} = \mu_Q \epsilon \epsilon_0 / \hbar$$

with  $\epsilon = k\sqrt{\hbar/(2M\omega_0)}$  and  $\epsilon_0 = k_0\sqrt{\hbar/(2M\omega_0)}$ , where  $\epsilon_0$  is normalized to one. This choice of parameters and scaling is useful for a number of reasons. It enable us to make a detailed comparison between the classical and quantum regimes. Note that the three parameters  $K$ ,  $\beta$  and  $\mu_{cl}$  are independent of  $\hbar$ . There are two important dynamical parameters,  $\mu_{cl}$  and  $\beta$ , and the parameter  $K$  which enables us to change the phase space periodicity of the system. This allows very small structures in the stochastic layer to be analysed without being hampered by the numerical precision of the computer used. For example, if  $K$  is fixed at 0.5 then the periodicity of the system is  $2\pi$ . However, if we change  $K$  to 0.001 then the system's periodicity becomes  $1000\pi$ , increasing the resolution of the phase space for analysis purposes. By making  $K$  small it is possible to magnify very small structures.

In what follows we will examine the dynamics of the system in detail, particularly in the resonant limit for the special case when the ratio  $\omega_0/\omega_1$  is  $\frac{1}{4}$ , where  $\omega_1 = 2\pi/\tau$ . As the dynamics are universal in the resonant case, this does not limit our conclusions. For the remainder of this paper  $K$  is kept at a constant value of 0.1 unless otherwise indicated.

### 3. Resonant kicking—analysis of the phase space orbit structure

The symmetry in the system's phase space depends solely on the value of the parameter  $\beta$ . The dramatic effect that the parameter  $\beta$  has on the phase space structure is illustrated in figures 1 and 2. In figure 1 we show the stochastic layer for  $\mu_{cl} = 6.5$ ,  $K = 0.1$  and  $\beta = \pi/2$ . The four-fold symmetry, determined by  $\omega_0/\omega_1$  being set at  $\frac{1}{4}$ , is clearly visible. In figure 2 the phase space structure is shown for the parameters  $\mu_{cl} = 6.5$ ,  $K = 0.1$  and  $\beta = (1 + \sqrt{5})\pi/2$ . This value of  $\beta$  is such that the frequency ratio is now incommensurate. In this non-resonant case there is no obvious long range symmetry. For the rest of the paper  $\beta$  is fixed at the resonant value of  $\pi/2$  and the phase space symmetry is four fold. We use the fourth return map (see the appendix) to locate the period-four fixed points of the system as these have a periodicity corresponding exactly with the phase space symmetry

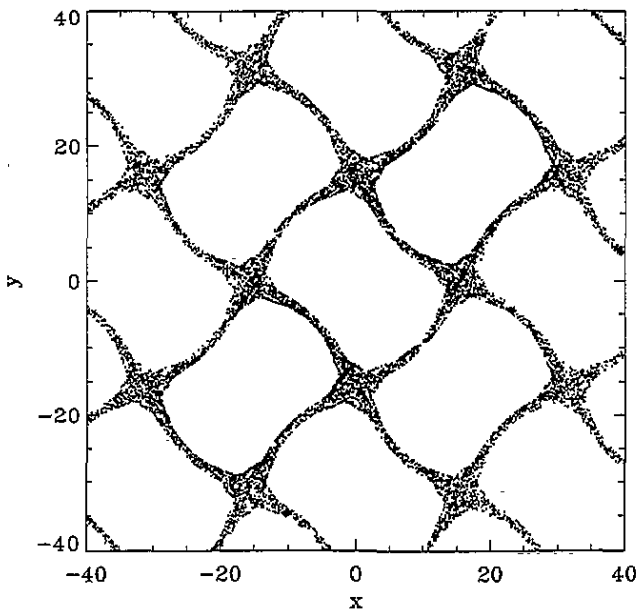


Figure 1. The stochastic layer at  $\mu_{cl} = 6.5$ ,  $K = 0.1$  and at resonance (i.e.  $\beta = \pi/2$ ).

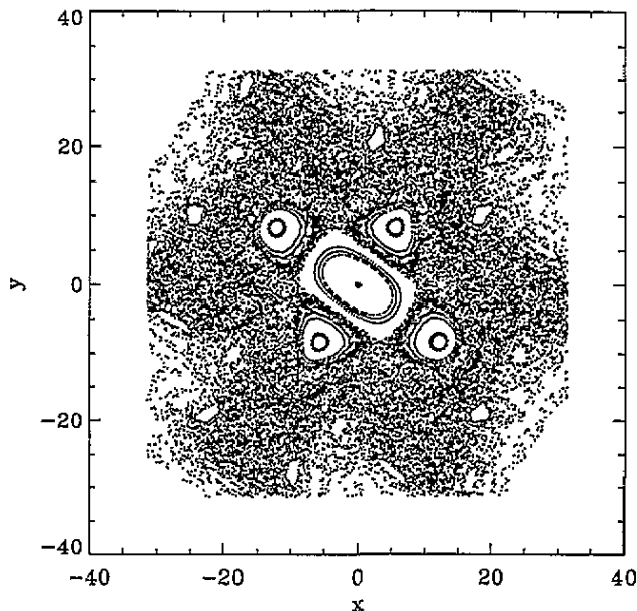


Figure 2. The phase space for  $\mu_{cl} = 6.5$ ,  $K = 0.1$  and  $\beta = (1 + \sqrt{5})\pi/2$ . The stochastic layer in this case has none of the web-like structure as for that at  $\beta = \pi/2$ . Some of the invariant orbits near the origin are shown for completeness.

for  $\beta = \pi/2$ . By direct calculation with this return map we find that all fixed points of period-four satisfy the condition

$$x = 5m\pi \quad y = 5n\pi \quad n, m \in \mathbb{Z} \quad (5)$$

As  $m$  and  $n$  can take on any integer value, the period-four points exist on a uniform grid which extends over the whole 2D plane of the phase space. The existence of this grid has far reaching consequences for the transport properties of certain phase space orbits. When  $m+n$  is an odd integer the  $x, y$  positions given in (5) correspond to a hyperbolic fixed point whose unstable and stable directions we denote by  $\lambda_+$  and  $\lambda_-$ , respectively. Explicit calculation of the  $\lambda$ 's for two adjacent hyperbolic fixed points  $A$  and  $B$ , with  $A = (5m\pi, 5n\pi)$  and  $B = (5(m+1)\pi, 5(n+1)\pi)$ , show that the unstable direction of  $A$  coincides with the stable direction of  $B$  and vice versa (see the appendix). We find that orbits in the vicinity of the unstable manifold of any hyperbolic period-four fixed point, say  $P1$ , can be shoved away to one of two neighbours,  $P2$  or  $P2'$ , because their stable manifolds are coincident with the unstable manifolds of  $P1$ . This is shown in figure 3. Once in the vicinity of  $P2$ , or  $P2'$ , the orbits are pushed away along their unstable manifolds to one of two of their neighbours and so the process continues until an orbit has visited all period-four hyperbolic fixed points in the 2D plane of the phase space. Therefore some orbits can spread (diffuse) out over the whole  $x$ - $y$  plane and it is these orbits that form the stochastic layer present in the system. To examine the orbit structure in more detail we recast the system Hamiltonian in terms of the standard action-angle variables,  $J$  and  $\theta$ . The new form for the system Hamiltonian  $H_T$  is

$$H_T(J, \theta) = H_0(J) + \mu_{cl}H_1(J, \theta) \quad (6)$$

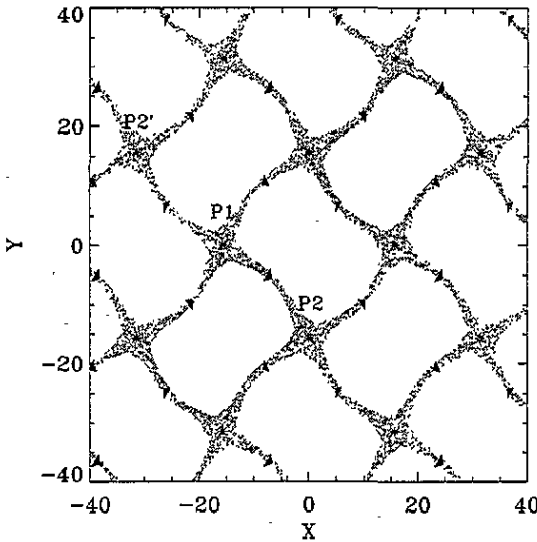


Figure 3. The period-four hyperbolic fixed points' manifold structure in the phase space for  $\mu_{cl} = 6.5$ ,  $K = 0.1$  and  $\beta = \frac{\pi}{2}$ . Each hyperbolic point lies at each intersection of the manifolds with the arrows indicating the direction of travel (pointing from means unstable and pointing to means stable). This structure is repetitive and covers the complete plane. The three labelled points,  $P1$ ,  $P2$  and  $P2'$ , are those referred to in the text. The stochastic layer is also included for comparison.

where

$$H_0 = J \quad \text{and} \quad H_1 = \cos(K\sqrt{J}\sin(\theta)) \sum_{n=-\infty}^{\infty} \delta(t - n\tau).$$

It consists of an integrable part  $H_0$  and a non-integrable part  $H_1$ . The system is certainly non-integrable for large values of  $\mu_{cl}$ , but, for the resonant case, we can ask the fundamental question: *to what extent is the system non-integrable for small non-zero values of  $\mu_{cl}$  and how does this non-integrability affect the invariant orbits in the phase space?*

For small values of the parameter  $\mu_{cl}$  the majority of orbits are unaffected by the kicking term. Detailed observations of the phase space, about the hyperbolic fixed point at  $(0, 5\pi)$ , show that the stochastic layer is very small and only those orbits with large  $H_1(J, \theta)$  have any discernible distortion. Therefore the level of non-integrability is very small and in most cases negligible. However, the term  $H_1(J, \theta)$  is not constant for fixed values of  $\mu_{cl}$ ,  $K$  and  $\beta$  and therefore those orbits with large  $H_1(J, \theta)$  can be sufficiently non-integrable to be distorted or destroyed altogether. This does, in fact, arise in the vicinity of the hyperbolic fixed points of period four and their corresponding manifolds. For sufficiently small perturbations of the integrable Hamiltonian the invariant orbits remain if the orbits have sufficiently incommensurate frequencies  $\omega_i$ . Those with commensurate frequencies or frequencies nearly commensurate do not remain unaffected but are distorted to a lesser or greater extent with some even being destroyed. The non-constant property of the  $H_1(J, \theta)$  term can negate, or even reverse, the effect of an increasing  $\mu_{cl}$  if the latter parameter is sufficiently small. In this case the non-integrable term becomes more of a perturbation and this seems to indicate that for sufficiently small  $H_1(J, \theta)$ , the effect on the Hamiltonian is similar to that of small  $\mu_{cl}$ .

We will now examine the case when  $\mu_{cl}$  is finite and beyond the perturbation realm. One would expect that if  $H_1(J, \theta)$  was of a sufficient size to be distorted when  $\mu_{cl}$  was small, then as  $\mu_{cl}$  is increased the distortion would increase and orbital (tori in higher dimensions) breakup would arise through an overlapping of higher resonance separatrices. This is indeed the case from observations of the phase space evolution. It should be noted that if  $H_1(J, \theta)$  is small enough to offset the increasing  $\mu_{cl}$  then the orbits would remain essentially undistorted as can be seen around the elliptic fixed point at the origin. Hence the larger the  $H_1(J, \theta)$  for any  $\mu_{cl}$  the greater the distortion and the sooner the breakup of the orbits. We find that the larger  $H_1(J, \theta)$  the more terms we need in the series expansion of the cosine term to accurately describe the behaviour. Therefore, more terms allow for higher-order periodic points and hence an earlier breakup of the orbits than for orbits with less terms and a smaller  $H_1(J, \theta)$  term.

What we have seen numerically above can also be seen analytically by taking the kicking term defined in (1) and (2), substituting for  $q$  with  $J$  and  $\theta$  and explicitly expanding out the kicking term to obtain

$$H_1(J, \theta) \equiv \sum_{m=0}^{\infty} (-1)^m \left( \frac{\hbar k^2}{M\omega_1} J \right)^m \frac{\sin^{2m}(\theta)}{(2m)!} \sum_{n=-\infty}^{\infty} \frac{\delta(t - n(2\pi/\omega_1))}{r^m} \quad (7a)$$

where  $\omega_0$  has been replaced by  $r\omega_1$ , where  $r = \omega_0/\omega_1$ . The above can be expressed in the more readable form

$$H_1(J, \theta) \equiv \sum_{m=0}^{\infty} (-1)^m f_m(J, \theta, \omega_1) \sum_{n=-\infty}^{\infty} g_{mn}(\omega_1, r) \quad (7b)$$

with the functions  $f_m(J, \theta, \omega_1)$  and  $g_{mn}(\omega_1, r)$  defined to be  $(\hbar k^2 J / M\omega_1) \sin^{2m}(\theta) / (2m)!$  and  $\delta(t - n(2\pi/\omega_1)) / r^m$ , respectively.

To analyse the behaviour of this system we need to consider the relationship between  $\omega_0$  and  $\omega_1$ . Remember that  $\beta = \pi/2$ , that is  $r = \frac{1}{4}$ . We have, in the function  $g_{mn}(\omega_1, r)$ , a way of describing the effect the relationship between  $\omega_0$  and  $\omega_1$  has on the existence of resonances in the complete system. It is evident from (7a) and (7b) that not only is the cosine term sampled by the delta function at a frequency  $\omega_1$  but also that this term has an infinite set of intrinsic frequencies,  $\omega_0^n (\equiv r^m \omega_1^n)$ , and that the ratio between these frequencies and  $\omega_1$  allows the various resonances to exist. We can use these resonances to predict the periodic points in the system's phase space. Thus, depending on the values chosen for  $m$ , the resonances allowed can be various and not just multiples of four. It is these resonances that cause the breakup of orbits in the phase space because only those orbits which are sufficiently incommensurate will survive an increase in the non-integrability of the system.

*How sufficient is sufficient?* This condition of sufficiency may become more apparent by examining the resonances for some low values of  $m$ . Table 1 shows how for a given value of  $m$ , the number of expected resonances is dependent on the number of factors of  $r^m$ . Furthermore, the statement 'maybe all factors which almost divide evenly into 256' used in table 1 implies that while there are multiples of 4 which do divide into its higher powers evenly, there can exist periodic orbits which have a periodicity close enough to a divisor of 256, or any power of  $4^m$ , with a small remainder. These constitute the quasi-commensurate orbits which accelerate the destruction of orbits with small  $\sqrt{J}$  whose resonances otherwise would be of insufficient number to breakup the orbits at the same value of  $\mu_{cl}$ . The periodic points actually observed in numerical simulations to date have

**Table 1.** The first few terms in the expansion of the driving term in (7) showing what resonances would be expected to be present. Those resonances shown in italics are those which nearly divide into the number given by  $r^m$ .

$m$	Resonances	$r^m \equiv (\omega_0/\omega_1)^m$
0	1-1	$\omega_1$
1	1-4 and 1-1	4
2	1-16, 1-8, 1-4, 1-1 <i>maybe a 1-5 and 1-3</i>	16
3	1-64, 1-32, 1-16, 1-8, 1-4, 1-1 <i>maybe 1-21, 1-13, 1-12, 1-9, 1-7, 1-5, 1-3</i>	64
4	All multiple of 4 up to 256 <i>maybe all factors which almost divide into 256 with small remainders</i>	256

been 1, 3, 4, 5, 6, 7, 8, 12, 16, 21, 24, 32, 48 and 72. The inherent difficulty of locating, numerically, fixed points of a specific periodicity is well known especially if the points sought have small Lyapunov exponents as this results in slow convergence to the points themselves [1]. Therefore the list presented above is as complete as permitted by the limit on computing time and by the resolution of the search grid used to locate the points.

The non-integrable cosine term,  $H_1$ , in the Hamiltonian, can only be expressed by its first few series terms when  $\sqrt{J} \sin(\theta)$  is small. As the  $\sqrt{J}$  can be considered, in the undriven oscillator, to be analogous to the radii of orbits in the driven case, for those orbits near the origin, we can make a similar identification. As the phase space has a definite four-fold symmetry then all invariant cells centred about a period-four elliptic point satisfying the condition in (5) can be transformed to the origin. Therefore we can presume that the contribution from the non-integrable term  $H_1$  about each of these elliptic fixed points is small. So  $\sqrt{J} \sin(\theta)$  tends to zero in the vicinity of the elliptic points of period four. The number of possible resonances in this region is small because of the small number of terms, in the cosine expansion of  $H_1$ , needed to adequately describe the system's behaviour (see table 1). Thus the possibility of orbital breakup is small for small values of the parameter  $\mu_{cl}$ , but becomes increasingly more probable as the kick strength  $\mu_{cl}$  is increased. The system is essentially integrable in these regions for small  $\mu_{cl}$ .

However, the further out we go from the elliptic fixed points at each invariant cell's centre then the more terms we require to satisfactorily describe the system's behaviour and hence the greater the number of possible resonances. There is a constant multiplier  $K$  in the  $H$  term which takes on the value 0.1 in the case being considered here. As a consequence of this the  $x$ 's and  $y$ 's have prominent fixed points every  $5\pi$  (as in (5)) with hyperbolic fixed points of period four at specific multiples of  $5\pi$  (see the appendix). The regions of the orbits nearest these hyperbolic points have the largest non-integrability and hence require the most terms in the cosine expansion of  $H_1$ . The most terms implies the greatest resonance overlap and for large  $\mu_{cl}$  their contributions can be very significant.

So the breakup of the orbits occur in the most non-integrable regions (that is regions where  $K\sqrt{J} \sin(\theta)$  is not small). For small  $\mu_{cl}$  the driving term (regardless of how many terms are in the cosine factor) is small and the system follows the scenario of commensurate orbital breakdown as described by the Kolmogorov-Arnold-Moser (KAM) theorem. As  $\mu_{cl}$  is increased the regions following this scenario contract about the elliptic fixed points described earlier. The outer regions for these large  $\mu_{cl}$  have many overlapping separatrices from each of the boundaries of the resonances. These overlapping separatrices breakup and form stochastic regions around the unbroken, albeit distorted, orbits. The width of the



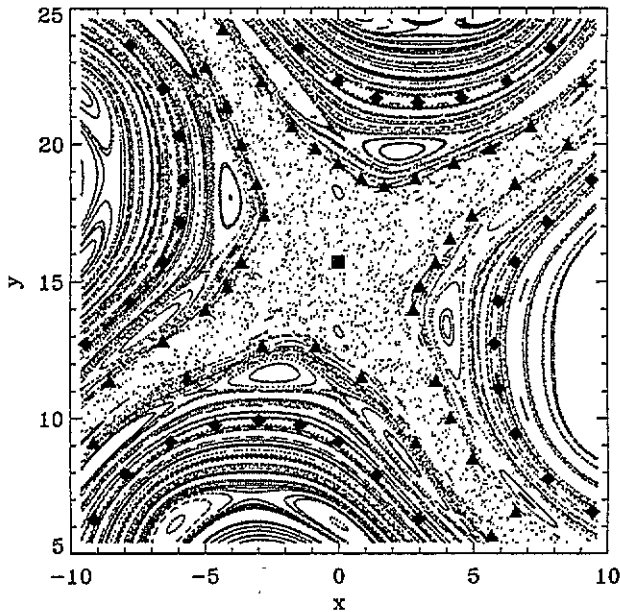


Figure 4. An enlargement of the phase space near the hyperbolic fixed point at  $(0, 5\pi)$  for  $\mu_{cl} = 6.5$ ,  $K = 0.1$  and  $\beta = \pi/2$ . The position of the period-four hyperbolic fixed point is highlighted by an opaque square while the positions of the period 24 and period 16 are highlighted with opaque triangles and diamonds, respectively.

stochastic region increases with increasing  $\mu_{cl}$  due to the contraction of the KAM regions about the elliptic fixed points.

We should expect even for very small  $\mu_{cl}$  the existence of a stochastic region around the hyperbolic points as these regions are the most non-integrable for any value of  $\mu_{cl}$ . As these regions contain the greatest number of possible resonances (due to the large  $J$  value) it follows that separatrix breakup into stochastic layers is very probable even at small  $\mu_{cl}$  values. The width of such a layer would be extremely thin and consequently would be very hard to locate numerically as the boundary would be quite sharp requiring high numerical precision. The way in which an increasing number of periodic points cause the breakup of the KAM orbits is clearly shown in figure 4, the phase space portrait for the mapping at  $\mu_{cl} = 6.5$  about the hyperbolic fixed point at  $[0, 5\pi]$ . It shows separatrices due to the presence of periodic points of increasing order as expected.

#### 4. Width of stochastic layer

We now undertake a detailed examination of the variation of the width of the stochastic layer as a function of the kick parameter,  $\mu_{cl}$ . Generally it is accepted that for small values of the driving parameter the width increases in an exponential manner [15, 16, 5]. To measure this width, a program was written which sampled points on the main  $x = 0$  axis through the hyperbolic fixed point  $(0, 5\pi)$  about which the layer exists. The width variation, for  $\mu_{cl}$  increasing from 0.1–3.0 inclusively, is shown in figure 5. The general trend seems to indicate an exponential increase with the data from the simulation fitting an exponential curve of the form

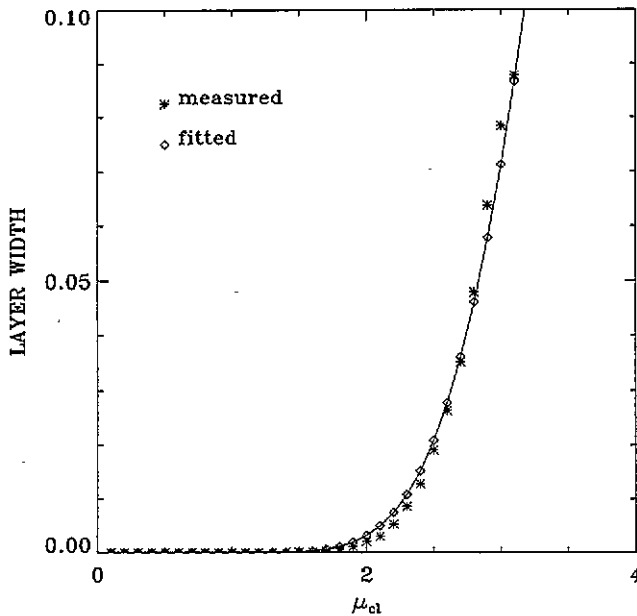


Figure 5. A graph of the normalized stochastic layer width against kick strength,  $\mu_{cl}$ , for  $K = 0.1$  and  $\beta = \pi/2$ . The asterisks denotes the measured values while the full curve (diamonds) denotes the fitted curve. The agreement is good but for values of  $\mu_{cl} > 3$  dips of increasing magnitude occur.

$$\Delta W = \frac{8\pi^3}{\mu_{cl}} \exp\left(-\sqrt{5} \frac{\pi^2}{\mu_{cl}}\right). \quad (8)$$

This form agrees exactly with that predicted analytically by Chernikov *et al* [16, 17, 18, 5]. (Note that the  $\sqrt{5}$  in the argument of the exponent arises from our explicit inclusion of  $K$  in our definition of  $\mu_{cl}$  in (3) and (4).)

For values of  $\mu_{cl}$  greater than 3.4, dips occur in the curve probably due to the presence of the periodic islands growing about high-order periodic points on the boundary where orbital breakup has occurred due to resonance overlap. These islands are evident only at values of  $\mu_{cl}$  greater than 3.0 and are considered to be the cause of the dips. The way in which a dip occurs is as follows: as the line along which the initial points for each set of iterations passes from the bounded orbital region to the stochastic region, it may encounter separatrices and periodic islands in its way. The separatrices may initially be bounded and hence non-stochastic but at some value  $\mu_{cl}$  become stochastic giving rise to a jump in the width curve. However, the islands may also increase in size pinching these regions and causing a dip with respect to the previous value if the program takes initial points that skip this region. The only way to measure the layer for the higher values is to plot the phase space, enlarge the boundary region and manually measure the region's width.

In the stochastic layer nearby points separate exponentially and have a positive Lyapunov exponent. This can be traced back to the manifolds for the period-four hyperbolic fixed points (see figure 3) along which orbits can diffuse over the whole phase space. Furthermore, depending on how near to, or on which side of, an unstable manifold an orbit is, determines on which unstable manifold it moves along at the next period-four hyperbolic point (as discussed previously). Thus nearby orbits can separate exponentially along this manifold structure. We have found that the calculated positive Lyapunov exponent (for a specific

orbit in the stochastic layer) versus  $\mu_{cl}$  follows a weighted average of the eigenvalues of the hyperbolic fixed points the orbits visits. The weighting depends on which point is visited and on which unstable manifold it leaves. For large  $\mu_{cl}$  the complexity of the layer and the proliferation of higher-order hyperbolic fixed points in this layer (brought about by invariant orbit breakup by overlapping resonances) brings about a variance in the above relationship between the Lyapunov exponent and the eigenvalues of the hyperbolic points. This variance is put down to the increased number of unstable manifolds from the higher-order hyperbolic fixed points bringing about a more complex motion in the layer than before. To our knowledge most of the analytic approaches to date have not taken into account these complexities.

### 5. Diffusion coefficient

We have previously mentioned how the orbits in the stochastic layer have a positive Lyapunov exponent so it is natural to investigate how the energy in this layer evolves in time. To accomplish this we calculate the mean energy for an ensemble of points in the stochastic layer. The results showed us that the growth in energy increases linearly with increasing  $n$  ( $n$  being the iteration counter and hence time) and so can be written as

$$E_n(\mu_{cl}, n) \equiv B(\mu_{cl})n \equiv B(\mu_{cl})\tau. \quad (9)$$

The dependence of this  $B$  parameter on the kick strength was itself examined to determine the dependence on  $\mu_{cl}$  unambiguously. It also was found to have a dependence close to that of  $\mu_{cl}^2$  with superimposed undulations. The dependence of the energy  $E_n$  on  $\mu_{cl}$  and  $n$  can be crudely approximated by

$$E_n(\mu_{cl}, n) \sim \mu_{cl}^2 n \equiv \mu_{cl}^2 \tau. \quad (10)$$

Care was taken in the above calculation to avoid using periodic points or quasi-periodic points as these points' non-diffuse behaviour would affect the result. These points were numerically filtered out. Having established the relationship between the mean energy in the layer and time, we can now use this result to determine how the diffusion coefficient  $D_{cl}$  varies as a function of the kick strength,  $\mu_{cl}$ .

The diffusion coefficient for a particular value of  $\mu_{cl}$  was measured by calculating the slope of the energy versus time graph, which from (9) is known to be linear. To alleviate problems associated with individual orbits and not the global nature of the system a set of 60 000 initial points were taken in the stochastic region close to one of the hyperbolic period-four fixed points. All points were tested for quasi-periodicity and iterated for 20 000 time steps. A graph of the numerical (simulated) results for the diffusion coefficient at  $K = 0.75$  is shown in figure 6 with the theoretical prediction (equation (11)) shown for comparison:

$$D_{cl}(\mu_{cl}) = \frac{1}{2}\xi^2\mu^2 \{1 - 2J_2(\xi\mu_{cl}) [1 - J_2(\xi\mu_{cl})]\} \quad (11)$$

where  $\xi = K_0/K$  and  $K_0 = 0.5$ . Note that when  $K = 0.5$ ,  $D_{cl}$  has the same universal form as that of the kicked rotator [10, 25]. The expression for  $D_{cl}$  in (11) was obtained using an approach similar to Rechester and White [25] in their study of the Chirikov–Taylor system with the only difference being our inclusion of the parameter  $\xi$  to account for our variable periodicity brought about by  $K$ . The behaviour of  $D_{cl}$  follows (11) over a large range of

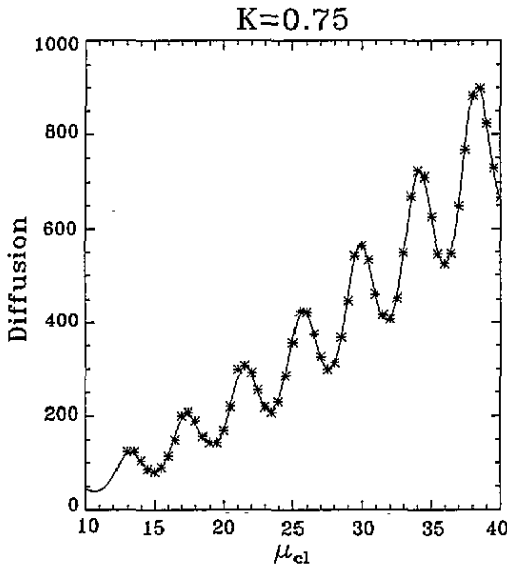


Figure 6. A graph of the diffusion coefficient,  $D_{cl}$ , versus the kick strength,  $\mu_{cl}$ , for  $K = 0.75$ . The asterisks represent the measured values while the full curve represents (11). The agreement is extremely good over a large range of the kick strength.

$\mu_{cl}$  before tending to a  $\mu^2$  dependence as  $\mu_{cl} \rightarrow \infty$ . This asymptotic limit was predicted by Chirikov for the kicked rotator [26]. The increased contribution from structure in the phase space for small kicks can be more easily examined using (11) than using the more usual form for  $D_{cl}$  because  $K$  can be used to magnify the phase space and hence to analyse small local effects by changing the phase space periodicity. Though  $K$  is not a *true* parameter (i.e. it has no physical analogue—it just changes the principle length scale of the problem) it does allow easier analysis of fine detail using numbers of a manageable magnitude without the numerical problems described earlier. The principle form of the deviation are spikes on the oscillations in the diffusion coefficient  $D_{cl}(\mu_{cl})$ . A detailed analytical study of these spikes is undertaken by Ishizaki *et al* for the kicked rotator [24]. By considering the influence of *accelerator modes* on the motion of orbits they show that  $D_{cl}$  diverges to infinity when the kick strength is close to integer multiples of the system's periodicity.

## 6. Conclusions

We have studied, in detail, the dynamics of the nonlinearly kicked oscillator at resonance. We have found for the kicked oscillator, at resonance, that the existence of periodic orbits in or around the stochastic layer influences the breakup of the invariant orbits as would be expected from the KAM theorem. Our analysis allows us to predict which resonances and hence which periodic orbits should be present in the system's phase space by means of a function obtained via a polynomial expansion of the kicking term. The correlation between prediction and numerical results was found to be very good despite the practical problems in numerically locating complete sets of periodic orbits.

We also studied the basic mechanism for transport in the stochastic layer, namely the diffusing of orbits along the (stable and unstable) manifolds of the period-four hyperbolic points whose separatrix net is the layer itself for infinitesimal kicking. A measure of the positive Lyapunov exponent for any diffuse orbit was found to match a weighted average of the magnitudes of the unstable manifolds of the orbits visited. Deviations at high kick values were found to result from a proliferation of other periodic orbits in the layer and gave a more complicated motion within the layer itself.

The detailed study of the evolution of the stochastic layer as the kick strength is increased is of fundamental importance as it enables us to see the effect of increasing non-integrability on the system at large. The most striking change in the layer is its variation in width with kick strength, which we studied in detail and compared to that predicted by perturbative analytical arguments [5]. We found that the width of the layer as a function of the kicking strength follows an exponential variation of the form  $u \exp(-u)$ , where  $u = 1/(\text{kickstrength})$ . This is the form predicted by Chernikov *et al* [5] for kick strengths  $\ll 1$ . We find that this result is true for a range of kick strengths considerably in excess of the theoretical prediction. This validity is surprising when one considers the increased complexity of the layer itself and the overall increase in structure at the layer boundary with increased kicking.

We have also measured the energy of the diffuse orbits within the layer as functions of both  $\mu_{cl}$  and time, and used these relationships to obtain the diffusion coefficient,  $D_{cl}$ , as a function of  $\mu_{cl}$ . The diffusion coefficient was subsequently measured over a range of the kick parameter and was shown to be oscillatory. The form of these oscillations was shown to be universal and, at resonance, to have the same form as that of the kicked rotator, but was found to extend over a larger range of  $\mu_{cl}$  than the corresponding analytical theory for the kicked rotator. Indeed, the lower asymptotic limit was found to be identical to that found by Lichtenberg and Wood who constructed an approximate theory of diffusion on the stochastic web which is valid in the small  $\mu_{cl}$  region [27].

### Acknowledgment

This work is supported by EOLAS, the Irish National Agency for Science and Technology.

### Appendix

In this appendix we illustrate how the fourth return map of the system allows us to predict the behaviour of all the period-four fixed points for a fixed set of the parameters  $K$ ,  $\beta$  and  $\mu_{cl}$ . The use of return maps is one of the standard methods of quantitatively examining and illustrating the symmetry of the system at a particular resonance value of  $\beta$ . This method is restricted, however, in that only positive integer ratios of  $\omega_0$  to  $\omega_1$  can have comparable return maps. Therefore if the ratio between  $\omega_0$  and  $\omega_1$  is  $n$  then the  $n$ th return map is required which exists only if  $n$  is a positive integer.  $\beta$ , in most of the analysis to follow, is fixed at  $\pi/2$  requiring us to obtain the fourth return map.

The fourth return map is that version of the classical mapping which relates  $y(n+1)$  to  $y(n-3)$ , not  $y(n)$ , and similarly  $x(n+1)$  to  $x(n-3)$ . Thus we can relate every fourth point explicitly. The fourth return map (denoted 4RM) is expressed thus

$$\begin{aligned} x(n+1) = & x(n-3) - \mu_{cl} \sin[2Ky(n-3) + 2K\mu_{cl} \sin(2Kx(n-3))] \\ & - \mu_{cl} \sin\{2Ky(n-3) + 2K\mu_{cl} \sin[2Kx(n-3)] + 2K\mu_{cl} \sin[2Kx(n-3) \\ & - 2K\mu_{cl} \sin[2Ky(n-3) + 2K\mu_{cl} \sin[2Kx(n-3)]]\} \end{aligned} \quad (A1)$$

$$\begin{aligned} y(n+1) = & y(n-3) + \mu_{cl} \sin[2Kx(n-3)] \\ & + \mu_{cl} \sin[2Kx(n-3) - 2K\mu_{cl} \sin[2Ky(n-3) + 2K\mu_{cl} \sin[2Kx(n-3)]]]. \end{aligned} \quad (A2)$$

The period-four fixed points are going to be those points satisfying the identities:

$$x(n + 1) = x(n - 3) \quad y(n + 1) = y(n - 3). \tag{A3}$$

So the solutions of (A3) are the fixed points of period four, two or one since any factor of four is a solution of the identity above. For a solution of the form  $x(n + 1) = x(n - 3)$  etc to occur all terms after the first on the right-hand side of (A1) and (A2) must go to zero. This means that all the sine arguments must all go to zero and so the period-four fixed points must satisfy

$$2Kx(n + 1) = 2Kx(n - 3) = 2Kx = m\pi \tag{A4}$$

$$2Ky(n + 1) = 2Ky(n - 3) = 2Ky = n\pi. \tag{A5}$$

As  $K$  has been chosen to be 0.1 for most of the analysis then it follows that the period-four fixed points are given by

$$x = 5m\pi \quad y = 5n\pi \tag{A6}$$

where  $n, m \in \mathbb{Z}$ . As  $m$  and  $n$  can assume any integer value then we must assume that these points exist in a uniform grid over the whole of the system's phase space.

Now that we have established this grid of points we need to consider whether these fixed points are hyperbolic or elliptic. The reason for this consideration is to determine in which regions of the phase space the unstable directions of the hyperbolic points exist as these determine the unbounded, diffuse behaviour evident in the system. To determine whether a periodic fixed point is elliptic or hyperbolic it is necessary to find its eigenvalues as given by the equation

$$|\mathbf{J} - \lambda \mathbf{I}| = 0 \tag{A7}$$

where, in this 2D mapping,  $\lambda$  is a 2D vector containing the eigenvalues,  $(\lambda_1, \lambda_2)$ ,  $\mathbf{J}$  is the Jacobian of the  $n$ th return map (where  $n$  is the periodicity of the fixed point) and is a  $(2 \times 2)$  matrix with  $\mathbf{I}$  the  $(2 \times 2)$  identity matrix.

The eigenvalues of an elliptical point form a complex conjugate pair such that the matrix  $\mathbf{M}$ , containing the eigenvalue solutions of (A7) for this specific fixed point, is a rotation matrix about the point itself. For a hyperbolic point its eigenvalues are not complex but real with the ratio between them such that their product is 1. In order for this condition to be satisfied, one eigenvalue must be greater than 1 with the other less than 1. Whichever eigenvalue is greater than 1 describes the unstable direction whereas the eigenvalue less than 1 describes the stable direction. To obtain these directions and to determine which points are hyperbolic we require the eigenvalue equation for the period-four fixed points of the system. To proceed further it is necessary to substitute, from (A6), the values of the period-four fixed points in order to eliminate the sin terms in the expressions for the 4RM. This substitution makes for a much simpler set of equations than those in (A1) and (A2). The Jacobian's elements,  $J_{ij}$  where  $1 \leq i, j \leq 2$ , can be found to be

$$J_{11} = \frac{\partial x(n + 1)}{\partial x(n - 3)} = 1 - 4K^2 \mu_{cl}^2 (-1)^{n+m} \tag{A8a}$$

$$J_{12} = \frac{\partial x(n + 1)}{\partial y(n - 3)} = 4K \mu_{cl} (-1)^n - 8K^3 \mu_{cl}^3 (-1)^{2n+m} \tag{A8b}$$

$$J_{21} = \frac{\partial y(n + 1)}{\partial x(n - 3)} = -4K \mu_{cl} (-1)^m + 8K^3 \mu_{cl}^3 (-1)^{2m+n} \tag{A8c}$$

$$J_{22} = \frac{\partial y(n + 1)}{\partial y(n - 3)} = 1 - 12K^2 \mu_{cl}^2 (-1)^{m+n} + 16K^4 \mu_{cl}^4 (-1)^{2(n+m)}. \tag{A8d}$$

The eigenvalue equation given previously, in (A7), now boils down to

$$\begin{aligned} & (1 - \lambda - 4K^2\mu_{cl}^2(-1)^{m+n})(1 - \lambda - 12K^2\mu_{cl}^2(-1)^{m+n} + 16K^4\mu_{cl}^4(-1)^{2(n+m)}) \\ & \quad - (4K\mu_{cl}(-1)^n - 8K^3\mu_{cl}^3(-1)^{2n+m})(-4K\mu_{cl}(-1)^n + 8K^3\mu_{cl}^3(-1)^{2m+n}) \\ & = 0. \end{aligned} \tag{A9}$$

This equation is solved on a computer using the formula for obtaining the roots of a quadratic equation to give the eigenvalues  $\lambda_+$  and  $\lambda_-$  for any period-four fixed point  $(5m\pi, 5n\pi)$  at specified values of  $\mu_{cl}$  and  $K$ . Remember that  $\beta$  is now fixed at  $\pi/2$ . It has been seen from results obtained numerically that for  $\mu_{cl} > 0$  the period-four fixed points with  $n + m$  odd are hyperbolic with unstable and stable directions given by  $\lambda_+$  and  $\lambda_-$ , respectively.

Furthermore, for two adjacent period-four hyperbolic points  $A$  and  $B$ , with  $A = (5m\pi, 5n\pi)$  and  $B = (5(m + 1)\pi, 5(n + 1)\pi)$ , the terms  $J_{21}$  and  $J_{22}$  for  $A$  are equal to  $-J_{21}$  and  $-J_{22}$ , respectively for  $B$ . The result of this is to cause the unstable direction of  $A$ , given by  $\lambda_+^A$ , to coincide with the stable direction of  $B$ , given by  $\lambda_-^B$ , and vice versa. This identity allows orbits to spread out over the entire phase space.

## References

- [1] Auerbach D, Cvitanovic P, Eckmann J, Gunaratne G and Procaccia I 1987 *Phys. Rev. Lett.* **58** 2387
- [2] Feigenbaum M, Jensen M and Procaccia I 1986 *Phys. Rev. Lett.* **56** 1503
- [3] Heller E J 1991 *Chaos and Quantum Physics* ed M J Giannoni, A Voros and J Zinn-Justin (Amsterdam: North-Holland) p 547
- [4] Gutzwiller M 1990 *Chaos in Classical and Quantum Mechanics* (New York: Springer)
- [5] Chernikov A A, Sagdeev R Z, Usikov D A and Zaslavsky G M 1989 *Sov. Sci. Rev. C Math. Phys.* **8** 83
- [6] Berman G P, Rubaev V Yu and Zaslavsky G M 1991 *Nonlinearity* **4** 543
- [7] Casati G, Chirikov B V, Israilev F M and Ford J 1979 *Stochastic Behaviour in Classical and Quantum Hamiltonian Systems* (Lecture Notes in Physics 93) ed G Casati and J Ford (Berlin: Springer) p 334
- [8] Israilev F M 1990 *Phys. Rep.* **196** 299
- [9] Zaslavsky G M, Zakharov M U, Sagdeev R Z, Usikov D A and Chernikov A A 1986 *Sov. Phys.-JETP* **64** 294
- [10] Dana I 1994 *Phys. Rev. Lett.* **73** 1609
- [11] Shepelyansky D and Sire C 1992 *Europhys. Lett.* **20** 95
- [12] Lima R and Shepelyansky D 1991 *Phys. Rev. Lett.* **67** 1377
- [13] Artuso R, Borgonovi F, Guarneri I, Rebuzzini L and Sire C 1992 *Phys. Rev. Lett.* **69** 3302
- [14] Daly M V and Heffernan D M to be published
- [15] Zaslavsky G M and Filonenko N N 1968 *Zh. Eksp. Teor. Fiz.* **54** 1590
- [16] Zaslavsky G M, Yu Zakharov M, Sagdeev R Z, Usikov D A, and Chernikov A A 1986 *Zh. Eksp. Teor. Fiz.* **91** 500
- [17] Chernikov A A, Sagdeev R Z, Usikov D A, Yu. Zakharov M and Zaslavsky G M 1987 *Nature* **326** 559
- [18] Chernikov A A, Sagdeev R Z, Usikov D A and Zaslavsky G M 1987 *Phys. Lett.* **125A** 101
- [19] Cohen D 1991 *Phys. Rev. A* **43** 639
- [20] Lu Zi-Min, Heagy J, Vallieres M and Yuan Jian-Min 1991 *Phys. Rev. A* **43** 1118
- [21] Schmera G, Jung P and Moss F 1992 *Phys. Rev. A* **45** 5462
- [22] D'Ariano G, Evangelista L and Saraceno M 1992 *Phys. Rev. A* **45** 3646
- [23] Kimball J, Singh V and D'Souza M 1992 *Phys. Rev. A* **45** 7065
- [24] Ishizaki M, Horita T, Kobayashi T and Mori H 1991 *Prog. Theor. Phys.* **85** 1013
- [25] Rechester A B and White R B 1980 *Phys. Rev. Lett.* **44** 1586
- [26] Chirikov B V 1979 *Phys. Rep.* **52** 265
- [27] Lichtenberg J and Wood P B 1989 *Phys. Rev. A* **39** 2153